# Undulations and Disorder in Block Copolymer Lamellae under Shear Flow

## H. Wang, P. K. Kesani, and N. P. Balsara*

*Department of Chemical Engineering, Polytechnic University, Six Metrotech Center, Brooklyn, New York 11201*

### B. Hammouda

*National Institute of Standards and Technology, Building 235, E 151, Gaithersburg, Maryland 20899*

ABSTRACT: The effect of shear flow on a concentrated block copolymer solution with lamellar microstructure was studied by *in-situ* small angle neutron scattering. Microstructural changes were determined from scattering measurements in all three principal directions (flow, velocity gradient, and neutral directions). The lamellae were found to align along the velocity direction but exhibited two orientations: one parallel to the shearing surfaces and the other perpendicular to the shearing surfaces. The perfection of the perpendicular alignment was always significantly greater than that of the parallel alignment. In fact, our sample in the parallel alignment was, to a large extent, disordered (i.e., liquid-like). In some cases, we found transient, well-aligned, perpendicular lamellae that eventually degenerated to poorly ordered, parallel lamellae. In one case, a systematic increase in lamellar undulations was evident prior to disordering. These results are not in agreement with current theories, which only predict enhanced order in block copolymers under shear flow.

## Introduction

The effect of flow fields on block copolymers continues to be an area of active research.[1−20] Recent interest in this field was triggered by the results of Koppi et al.,[4] who reported that diblock copolymer lamellae under shear flow can either lie *parallel* to the shearing plates or stand up *perpendicular* to them, depending on shear rate and temperature. Of course, in the absence of shear and other external fields, all lamellar orientations are equally likely, and one obtains an isotropic orientation distribution function. The three situations are depicted schematically in Figure 1. At that time, the perpendicular alignment was not anticipated, and a plausible explanation for this result was proposed by Koppi et al. They speculated that lamellar undulations caused by the vorticity of the shear field would cause the parallel alignment to be unstable relative to the perpendicular alignment.

In the intervening years it has become clear that the problem is more complicated than originally envisioned. In a typical experiment one puts a block copolymer in a shearing apparatus, heats it above the quiescent order to disorder transition (to erase thermal and shear history), cools it to a specified temperature ($T$), waits for some amount of time ($t_{wait}$), and then applies a periodic shear field with a fixed frequency ($\omega$) and amplitude ($A$). It has now become clear that the final alignment depends on all four variables ($T$, $t_{wait}$, $\omega$, and $A$).[4−16] Further, the conditions under which different alignments are observed change qualitatively from sample to sample. For instance, in polystyrene-*block*-polyisoprene copolymers, the parallel alignment is achieved at high frequencies and low temperatures, while in poly(ethylenepropylene)-*block*-poly(ethylethylene) copolymers, the parallel alignment is achieved at low frequencies and high temperatures. Several of the experimental results reported in ref 4−16 are not explained by current theories.[17−20]
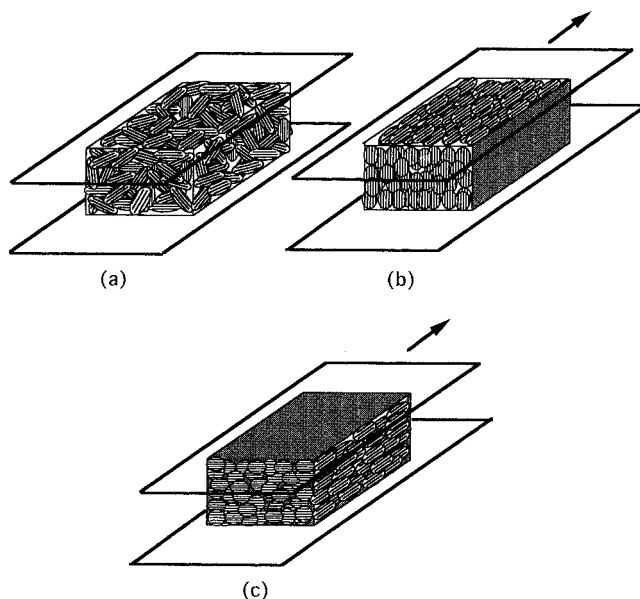
**Figure 1.** Schematic view of commonly encountered, lamellar orientations in block copolymers under shear flow. The arrow indicates the direction in which one of the confining plates is translated: (a) isotropic distribution of orientations and (b and c) anisotropic distribution of orientations with lamellae oriented along the flow direction (b) perpendicular (to the shearing plates) and (c) parallel (to the shearing plates).

In some experiments,[1,2,4,5,8,10,11,15] microstructural orientation was determined in a separate apparatus after applying the shear field, while in others,[6,7,9,12−14,16] this determination was made *in-situ* while the shear field was applied. The *in-situ* experiments enable studies of microstructural evolution under shear. In most cases, shear fields cause a monotonic change from the unaligned state to the aligned state.[7,9,12−16] A more interesting result was obtained by Gupta et al., who showed that the lamellar alignment in a diblock copolymer sample changed first from isotropic to perpendicular and then from perpendicular to parallel.[6] The importance of intermediate states was not previously recognized.

The presence of defects and imperfections in shear-aligned samples is expected. Like other smectic A systems,[21,22] lamellar block copolymers obtained after a quiescent quench consist of coherently ordered regions or "grains", with concomitant discrete (points, lines, and walls) and continuous (texture) defects.[23,24] It is reasonable to assume that some of these defects will persist under shear. Other factors such as imperfect alignment of the shearing surfaces on the length scale of the microstructure[25] and thermal fluctuations[13] may also cause defects in microstructure alignment. In addition to alignment defects, the application of a shear field may adversely affect the order within each grain. Both theory and experiment have shown that increasing shear rate increases the order to disorder transition temperature in diblock copolymers.[9,14,16,17–20] This implies that turning on the shear field at a given temperature in the ordered state should result in a larger quench depth [quench depth = (sample temperature) − (order to disorder transition temperature)], i.e., better defined lamellae with sharper interfaces. We thus expect shear fields to produce enhanced order within each grain, relative to the quiescent state.

In this paper we present *in-situ* small angle neutron scattering measurements of lamellar alignment in a concentrated diblock copolymer solution under a periodic shear field. We pay particular attention to the imperfect nature of the shear-aligned state. The sample exhibited parallel and perpendicular orientations in the accessible frequency and temperature window. We studied the reorganization from the quiescently quenched state to both states. We also studied the perpendicular to parallel transition, which could be initiated at a fixed temperature by increasing frequency. A systematic difference in defect density was found when parallel and perpendicular alignments were compared. In fact, we show that under shear, our sample in the parallel alignment was, to a large extent, disordered. Thus, the application of shear can adversely affect the order within individual grains. This observation is in dissonance with current theories on the effect of flow on ordered diblock copolymers.[17–20] In some cases, we found transient, well-aligned perpendicular lamellae that eventually degenerated to the poorly ordered, parallel lamellae. In one particular case, the disordering was caused by an undulation instability.

## Experimental Details and Data Analysis

A polystyrene−polyisoprene diblock copolymer was synthesized by anionic polymerization under high vacuum. The weight-average molecular weights of the polystyrene and polyisoprene blocks were determined to be 16.0 and 18.4 kg/mol, respectively, polydispersity index of the copolymer = 1.07, and we refer to this polymer as SI(16−18). Polymer characterization methods are given in ref 26. Experiments were conducted on a 55 wt % solution of SI(16−18) in distilled[9] dioctyl phthalate (DOP). No deuterium labeling was necessary due to the natural neutron contrast between polystyrene and polyisoprene. The quiescent order to disorder (ODT) transition temperature of this solution was measured by the local birefringence method[27,28] and found to be 35 ± 1 °C. It is expected that the DOP will be uniformly distributed throughout the sample. The volume fraction of polystyrene in the copolymer is 0.53. We expect a lamellar phase below 35 °C and a liquid-like, disordered phase above 35 °C. No order−order transitions are expected, based on current knowledge.[29–31] The experimental results presented here are in agreement with this expectation.

The solution was placed in a shear cell consisting of two concentric quartz cylinders, an outer rotor, and an inner stator.
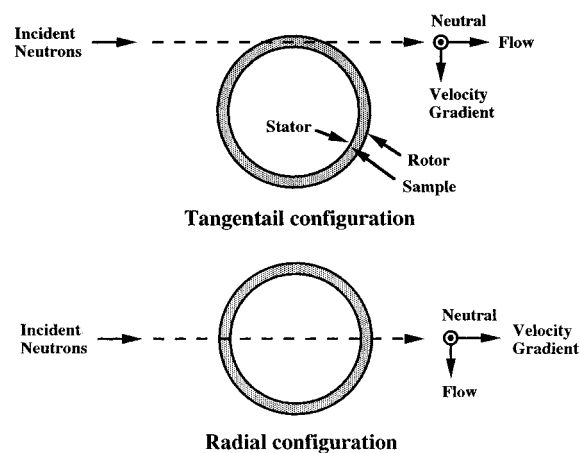


**Figure 2.** Schematic of the top view of the shear cell in tangential and radial configurations.

The gap between the two cylinders was 0.5 mm, and the motion of the rotor was computer controlled. A periodic shear field was imposed on the sample, where the time dependence of the rotor displacement had a triangular wave form. Following Koppi et al.,[4] we call this a reciprocating shear field. Neutrons with a wavelength of 0.6 nm were directed at the shear cell using a vertical 2 mm × 12 mm slit as the sample aperture (see ref 9 for instrument configuration and other details). The shear cell was mounted on a translation stage and could therefore be moved relative to the incident beam. We used two instrument configurations: one where the beam was directed through the center of the cell, which we refer to as the radial configuration, and the other where the beam was directed through the edge of the cell, which we refer to as the tangential configuration. A schematic of the instrument is shown in Figure 2. We thus obtained the scattering profiles in two planes. The scattering profile in the flow−neutral plane was obtained in the radial configuration, while that in the velocity gradient−neutral plane was obtained in the tangential configuration. The SANS experiments were conducted on the NG3 beam line at the National Institute of Standards and Technology (NIST) in Gaithersburg, MD, and the shear cell was built by G. C. Straty at NIST in Boulder, CO.

Before starting each experimental run, the sample history was erased by heating the sample to 39 °C for 30 min. The sample was then cooled to a predetermined temperature in the ordered state (below 35 °C). The cooling process took about 20 min. We waited for 10 min after the sample temperature had stabilized and then commenced shearing the sample at a predetermined amplitude and frequency. In all cases the strain amplitude was 400%. In the remainder of the paper, the shear field is specified by the frequency, $\omega$ (rad/s). The shear rate during each stroke of the reciprocating shear cycle is constant and equal to $4\omega/\pi$ (1/s). Time zero is defined as the time at which the shearing was commenced. Small angle neutron scattering (SANS) intensity profiles were measured in time slices of 3 min. In most experiments, the shear cell was manually translated back and forth from the radial to the tangential configuration between measurements. It took 1 min to translate the shear cell from one configuration to the other, and no data were recorded during this period. We were thus able to monitor the evolution of both radial and tangential scattering profiles during shear alignment. In a few cases, the shear cell was left in one configuration throughout the run. These experiments confirmed that translation of the cell did not introduce any artifacts. The SANS intensity, normalized to a constant monitor count ($10^8$), were corrected for background scattering and are reported as a function of $\mathbf{q}$, the scattering vector, $|\mathbf{q}| = 4\pi \sin(\theta/2)/\lambda$, where $\theta$ is the scattering angle and $\lambda$ is the wavelength of incident beam ($\lambda = 0.6$ nm).

Typical two-dimensional scattering data obtained from the SI(16−18)/DOP solution, in the tangential configuration, are shown in Figure 3a,b in the form of isointensity contour plots. The data in Figure 3a (obtained after 3 min of shearing at $T$ = 26.9 °C and $\omega$ = 5.0 rad/s) indicate perpendicular alignment
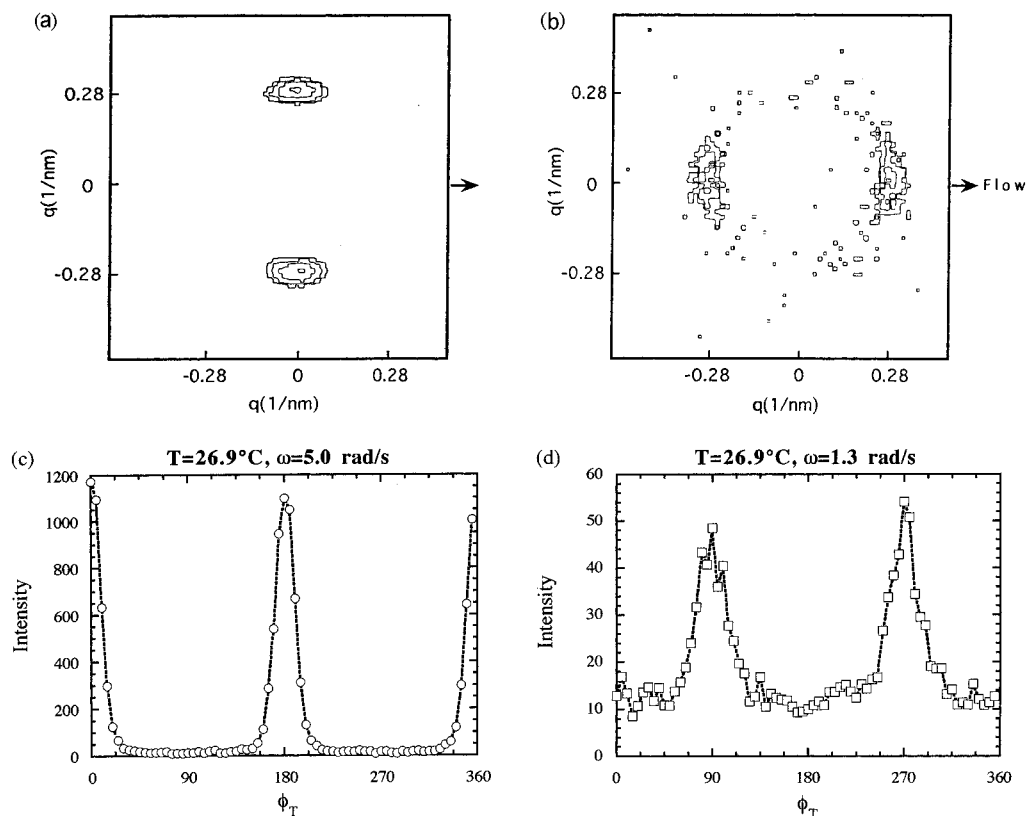
**Figure 3.** (a and b) Representative 2-D plots of isointensity contours at the $T = 26.9$ °C in the tangential configuration after shearing (a) for 3 min at $\omega = 5.0$ rad/s and (b) for 37 min at $\omega = 1.3$ rad/s. (c and d) Same data, converted to 1-D, ring-averaged plots of intensity versus azimuthal angles in the tangential ($\phi_T$) and radial ($\phi_R$) planes: (c) same as panel a and (d) same as panel b.

of the lamellae, while the data in Figure 3b (obtained after 30 min of shearing at $T = 26.9$ °C and $\omega = 1.3$ rad/s) indicate parallel alignment. The scattering peaks were located at $|\mathbf{q}| = 0.28 \pm 0.01$ nm$^{-1}$, regardless of shear field and temperature, indicating a constant interlamellar spacing of $22.4 \pm 0.1$ nm. It is evident that most of the scattered intensity is restricted to a ring defined by 0.244 (1/nm) $\leq |\mathbf{q}| \leq$ 0.324 (1/nm). This was found to be true regardless of temperature, shear field, and instrument configuration. Consequently, no information is lost when the data are converted to one-dimensional plots of the integrated intensity in the ring, 0.244 (1/nm) $\leq |\mathbf{q}| \leq$ 0.324 (1/nm), as a function of the azimuthal angle in the scattering plane. We use $\phi_R$ to denote the azimuthal angle in the flow−neutral plane (radial configuration) and $\phi_T$ to denote the azimuthal angle in the velocity gradient−neutral plane (tangential configuration). Both angles are measured with respect to the neutral direction. In Figure 3c,d we show the ring-averaged profiles corresponding to the two-dimensional data shown in Figure 3a,b, respectively.

In Figure 4 we show ring-averaged, radial and tangential scattering data obtained after a quiescent quench from the disordered state to 24.4 and 26.9 °C. It is evident that the quiescent quench to 24.4 °C produces an anisotropic distribution of lamellae. The tangential view indicates that the volume fraction of lamellae oriented parallel to the shearing surfaces is significantly greater than that in other directions accessible in this configuration. Similarly, the radial profile indicates a slight bias for the layer normals to lie perpendicular to the flow direction in spite of the fact that the flow field has not yet been imposed. This is undoubtedly the effect of finite sample thickness (0.5 mm in this case). The anisotropy of layer orientations obtained under quiescent conditions decreases with increasing temperature, and no anisotropy was evident after the quiescent quench to temperatures greater than or equal to 26.9 °C (Figure 4).

Our objective is to quantify the microstructural changes in different directions while imposing shear. We do so by using the data obtained in the isotropic state, before turning on the
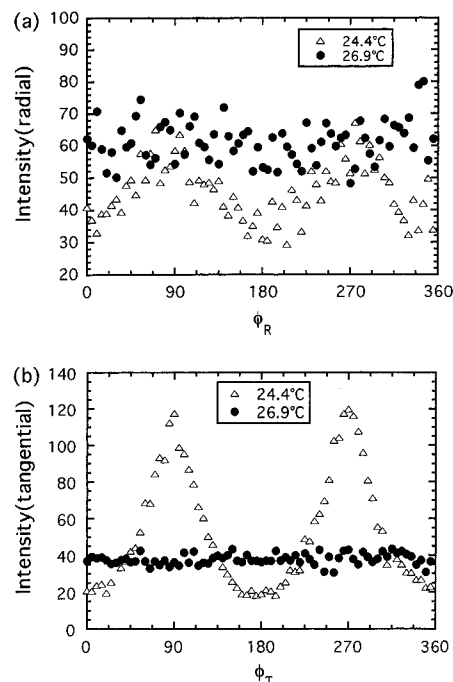


**Figure 4.** Scattering intensity profiles in (a) radial and (b) tangential planes, obtained after a quiescent quench from 39 to 26.9 and 24.4 °C.

flow, to normalize the measured intensity profiles under flow. The magnitude of the peak intensity (at $|\mathbf{q}| = 0.28$ nm$^{-1}$), obtained by our experimental protocol under quiescent conditions, was a weak function of temperature between 26.9 and 39.0 °C (10% change), in spite of the ODT at 35 °C. This is expected due to the relatively short annealing times that were used.[32] The temperature window over which we examined the effect of shear on this sample was relatively small: from 24.0

**Table 1. Summary of Final Lamellar Alignment Obtained in SI(16−18)/DOP under Reciprocating Shear, Starting from the Quiescently Quenched State**

| $T$ (°C) | $\omega = 0.16$ rad/s | $\omega = 0.63$ rad/s | $\omega = 1.3$ rad/s | $\omega = 2.5$ rad/s | $\omega = 5.0$ rad/s |
|---|---|---|---|---|---|
| 24.0 | | | | parallel | |
| 24.4 | parallel | parallel | | | |
| 25.2 | perpendicular | | | | |
| 26.9 | perpendicular | | parallel | | parallel |

to 26.9 °C. The isotropic peak intensity in this temperature range is estimated to be 38.2 ± 0.8 units for the tangential profiles and 61.4 ± 1.2 units for the radial profiles, based on extrapolations of the scattering profiles obtained between 26.9 and 39.0 °C. The extrapolations were necessary because quiescent quenches to temperatures below 26.9 °C gave anisotropic scattering profiles. In the discussions that follow, we normalize the ring-averaged, tangential and radial intensities by 38.2 and 61.4 units, respectively. We use the symbols $I_T$ and $I_R$ to indicate normalized, ring-averaged, tangential and radial intensities, respectively. This normalization accounts for differences in the scattering volume and transmission coefficient in the radial and tangential configurations.

The small angle scattering intensity in a given direction in the scattering plane is dominated by scattering from lamellae with normals coincident with that direction. If we assume that the sample is composed of ordered grains at various locations, **r**, whose orientations are described by unit normals, **n(r)**, perpendicular to the lamellae at **r**, then the normalized scattered intensity is approximately given by

$$I_i(\mathbf{q}) \sim c(\mathbf{n})\, f(\mathbf{n})\, \delta(\mathbf{q}/|\mathbf{q}| - \mathbf{n}) \ (i = R \ or \ T) \qquad (1)$$

where $c(\mathbf{n})$ is the average scattering power grains with orientation **n** and is related to the order within each grain, $f(\mathbf{n})$ is the volume fraction of grains with orientation **n**, and $\delta$ symbolizes the delta function. If we assume that the shear field does not affect the order within the grains, then the normalized scattering intensities monitor the increase or decrease of the volume fraction of ordered grains with normals oriented along **q**. Thus the scattered intensity at $\phi_T = 0°$ and 180° is proportional to the volume fraction of perpendicular lamellae, while the scattered intensity at $\phi_T = 90°$ and 270° is proportional to the volume fraction of parallel lamellae. Similarly, the scattered intensity at $\phi_R = 0°$ and 180° is proportional to the volume fraction of perpendicular lamellae, while the scattered intensity at $\phi_R = 90°$ and 270° is proportional to the volume fraction of transverse lamellae. We define the transverse orientation of the lamellae to be one that is orthogonal to both perpendicular (Figure 1b) and parallel (Figure 1c) lamellae. Our measurements permit us to quantify the time dependence of alignment in all three principal directions—flow, velocity gradient, and neutral directions, and we obtain redundant information regarding the volume fraction of perpendicular lamellae from the radial and tangential profiles.

## Results and Discussion

We now discuss structural changes in the sample caused by the imposition of reciprocating shear. In Table 1 we list the temperature and frequency dependence of the "final" lamellar orientations (after about 40 min of shearing). Even though only two final states were found, the kinetics of the transition from the quiescently quenched state to the aligned state depended strongly on temperature and frequency.

**Effect of Frequency at 24.4 °C.** We begin by describing results obtained at 24.4 °C and $\omega = 0.16$ rad/s. In Figure 5 we show the tangential results at selected times ($t$) after turning on the shear field, in the form of normalized intensity, $I_T$, versus $\phi_T$. It is evident that imposition of the shear field produces little change in lamellar alignment. The lamellae were predominantly
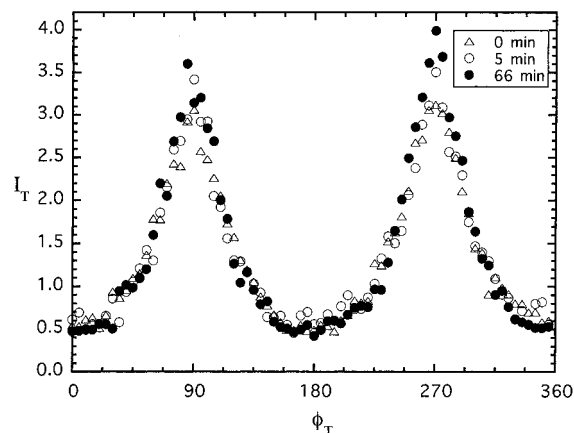


**Figure 5.** Evolution of the tangential scattering profile ($I_T$ versus $\phi_T$) with time while shearing at 24.4 °C with $\omega = 0.16$ rad/s. The shear field has little effect on lamellar orientation under these conditions.

in the parallel orientation after a quiescent quench, and shearing for 1 h results in a slight increase in the volume fraction of parallel lamellae. Note that the final alignment obtained at 24.4 °C and $\omega = 0.16$ rad/s is due entirely to finite gap effects; the shear field played no part in determining alignment. If we were to use a larger gap size, the orientation anisotropy after the quiescent quench would probably be less. This would imply a different initial condition, which, in all probability, would lead to a different final condition. Our experiments indicate that the walls of typical shear cells can exert a significant "field" on the lamellae. In some cases, this field can dominate, making the shear field irrelevant. The necessity of quantifying the orientation of both initial and final states in a shear alignment experiment is obvious.

The kinetics are more interesting when $\omega = 0.63$ rad/s is imposed on the sample at 24.4 °C. As always, the sample was disordered prior to the run. The time dependence of the radial profile is shown in Figure 6a. Three minutes after the imposition of shear, most of the transverse lamellae were eliminated, leaving behind an excess of lamellae with perpendicular orientation. The resulting profile has sharp peaks at $\phi_R = 0°$, 180°, and 360°. The normalized peak intensity ($I_R$) at these angles is in the vicinity of unity (about 1.3). On the other hand, $I_R(\phi_R = 90°, 270°)$ was only 0.2. As time proceeds, the perpendicular lamellae are also eliminated and $I_R$ reaches an asymptotic value of 0.2 at all values of $\phi_R$.

If we assume that the shear field only reorients existing grains and that it does not adversely affect the order within the grains, the data in Figure 6a would imply that at $t = 36$ min, at least 80% of the lamellae with perpendicular and transverse orientation at $t = 0$ have been reoriented. We expected these lamellae to lie in the parallel orientation because all previous experiments and theories on shear alignment[1−20] had yielded parallel or perpendicular orientations. This implies that $I_T(\phi_T = 90°, 270°)$ should be greater than unity. The time evolution of the tangential profiles, shown in Figure 6b, allows us to test our hypothesis. Initially (at $t = 0$) we see an excess of parallel lamellae, which are eliminated during the initial stages of alignment. In 16 min, $I_T(\phi_T = 90°)$ decreases from 2.5 to about 1. Surprisingly, the perpendicular lamellae stayed intact during this period, and at $t = 16$ min, the two-dimensional scattering profile contained four spots, indicating the coexistence of parallel and perpendicular
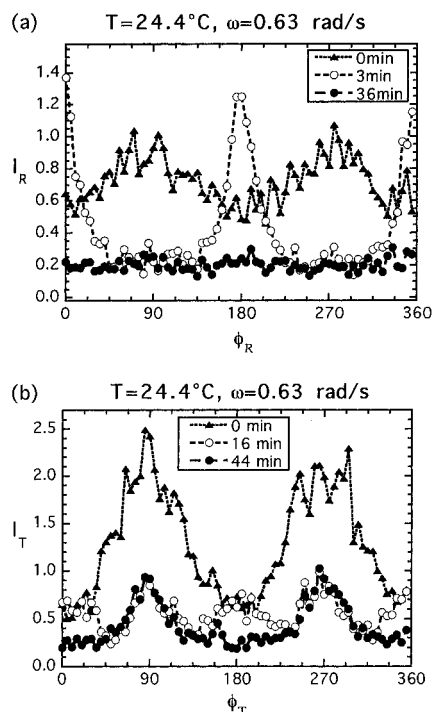
**Figure 6.** Evolution of normalized (a) radial and (b) tangential scattering with time while shearing at 24.4 °C with $\omega = 0.63$ rad/s.

lamellae. Beyond this point, there was no further elimination of parallel lamellae, and the intensity due to the perpendicular lamellae, $I_T(\phi_T = 0°, 180°)$, decreased to a value of 0.2.

After 44 min of shearing, we are left with an intensity of 1 in the velocity gradient direction and 0.2 in all other accessible directions. The fact that $I_T(\phi_T = 90°, 270°)$ is not significantly greater than unity is inconsistent with our expectation. Therefore, our assumption that the shear field does not adversely affect the order within the grains must be incorrect. We are forced to conclude that the shear field has caused the disordering of all ordered grains except those in the parallel orientation. Further, the concentration fluctuations in these disordered regions under shear must be strongly suppressed, relative to the quiescent state. Note that the quiescent scattering intensity due to disordered concentration fluctuations at 39 °C is only 10% lower than what we observed in the ordered state at 24.4 °C. Therefore, if the concentration fluctuations in shear-disordered regions at 24.4 °C were of the same amplitude as those at 39 °C, then $I_R$ would be 0.9. The fact that we obtain 0.2 indicates that the amplitude of the concentration fluctuations is much lower than that at 39 °C. By extrapolating our data, we estimate that the amplitude of the concentration fluctuations in the shear-disordered regions is similar to that obtained at 150 °C under quiescent conditions. Unambiguous determination of the mostly disordered nature of the sample would not have been possible if the concentration fluctuations were not suppressed to such a large extent.

The response of the SI(16−18)/DOP sample to $\omega = 0.63$ rad/s at 24.4 °C is summarized in Figure 7 where we plot the time dependence of the scattered intensity in the principal directions, which, as mentioned above, is proportional to the volume fraction of lamellae with normals oriented in these directions. Note the consistency of the perpendicular lamellae volume fraction obtained independently from the radial and tangential profiles.
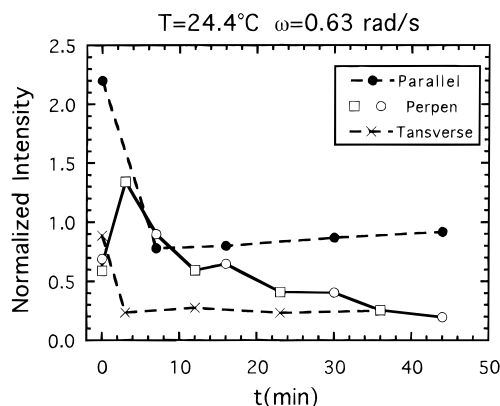


**Figure 7.** Time dependence of the normalized intensities in the principal directions at 24.4 °C with $\omega = 0.63$ rad/s. As indicated in the text, these values reflect the increase or decrease in the volume fraction of lamellae with normals in the corresponding, principal directions: (○) $I_R(\phi_R = 0°, 180°)$ or volume fraction of perpendicular lamellae estimated from the radial profiles, (□) $I_T(\phi_T = 0°, 180°)$ or volume fraction of perpendicular lamellae estimated from the tangential profiles, (×) $I_R(\phi_R = 90°, 270°)$ or volume fraction of transverse lamellae estimated from the radial profiles, and (●) $I_T(\phi_T = 90°, 270°)$ or volume fraction of parallel lamellae estimated from the tangential profiles.
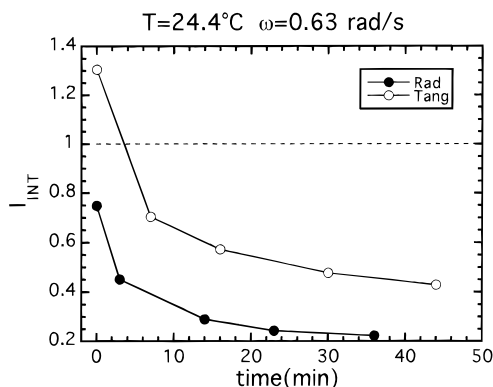


**Figure 8.** Time dependence of the integrated intensities, $I_{INT}$, corresponding to the radial and tangential scattering profiles while shearing at 24.4 °C and $\omega = 0.63$ rad/s.

Thus far we have focused on lamellae oriented along the principal directions. The decrease in the volume fraction of lamellae in these directions could, in principle, be due to a slight misalignment of grains. To rule out this possibility we computed $I_{INT}$, the integrated intensities corresponding to the radial and tangential, ring-averaged profiles:

$$I_{INT} = \frac{1}{2\pi}\int_0^{2\pi} I_i(\phi_i)\, d\phi_i \ (i = R \text{ or } T) \tag{2}$$

The time dependence of $I_{INT}$ is shown in Figure 8. After 45 min of shearing, $I_{INT}$ corresponding to both radial and tangential profiles decreased to values that are significantly lower than unity. This an unambiguous signature of shear disordering, i.e., a dramatic decrease in the scattering power of ordered grains [$c(\mathbf{n})$].

In the above analysis we have implicitly assumed that normals to the lamellae do not lie in planes that are inaccessible to us. This is a reasonable assumption, based on current understanding. In fact, current theories indicate that lamellar normals under shear must be confined to the neutral−velocity gradient plane.[17−20,33] This is because deformation of lamellae along the layer normals implies a change in interlamellar spacing away
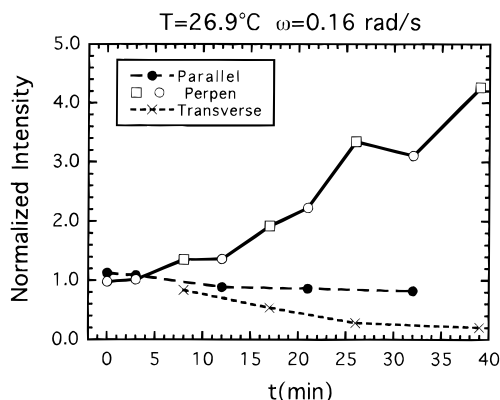
**Figure 9.** Time dependence of the normalized intensities in the principal directions at 26.9 °C with $\omega = 0.16$ rad/s. As indicated in the text, these values reflect the fractional enhancement of the volume fraction of lamellae with normals in the corresponding, principal directions: (O) $I_R(\phi_R = 0°, 180°)$ or volume fraction of perpendicular lamellae estimated from the radial profiles, ($\square$) $I_T(\phi_T = 0°, 180°)$ or volume fraction of perpendicular lamellae estimated from the tangential profiles, ($\times$) $I_R(\phi_R = 90°, 270°)$ or volume fraction of transverse lamellae estimated from the radial profiles, ($\bullet$) $I_T(\phi_T = 90°, 270°)$ or volume fraction of parallel lamellae estimated from the tangential profiles.

from the equilibrium value. Any grains whose normals have a non-zero component along the flow direction must suffer such deformations. The interlamellar spacing in lamellar block copolymers is determined by a sharp minimum in the free energy,[29−31,33] and thus any deviations from this value are subject to a large free energy penalty. On the other hand, this penalty is not shared by lamellae whose normals are orthogonal to the flow direction, i.e., in the neutral−velocity gradient plane. It is therefore highly unlikely that lamellae with normals not confined to the neutral−velocity gradient will survive for a significant amount of time under shear. The data obtained in the radial configuration are in agreement with this view (Figure 6a). After 3 min of shearing, all the lamellae, except those with normals in the neutral direction, were expunged.

**Effect of Temperature at $\omega = 0.16$ rad/s.** We saw in the preceding section that at $T = 24.4$ °C imposing a shear field with $\omega = 0.16$ rad/s had no effect on lamellar alignment (Figure 5). In Figure 9 we show the evolution of normalized intensities along the principal directions after imposing the same frequency at $T = 26.9$ °C. We now see a transformation from a nearly isotropic alignment to a predominantly perpendicular alignment. Note that the normalized scattering intensities corresponding to the perpendicular alignment are in the vicinity of 4 after 40 min of shearing. This implies that the volume fraction of perpendicular lamellae is increased by 300%, relative to the quiescent, isotropic state. In that period, the shear field produces a 10% reduction in the parallel lamellae volume fraction [$I_T(\phi_T = 90°, 270°) = 0.9$] and an 80% reduction in the transverse lamellae volume fraction [$I_R(\phi_R = 90°, 270°) = 0.2$]. The time dependence of $I_{INT}$ for this case is shown in Figure 10. After 35 min of shearing, the integrated tangential intensity increases by about 30% while the integrated radial intensity decreases by the same amount. It is evident from the data shown in Figures 9 and 10 that the alignment of the lamellae under these conditions is quite imperfect. We, however, do not see clear signs of shear disordering, as we did at $T = 24.4$ °C and $\omega = 0.63$ rad/s.
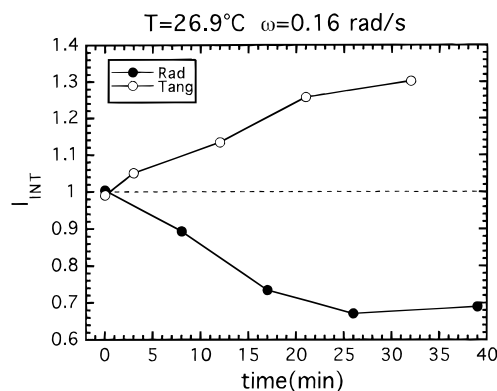


**Figure 10.** Time dependence of the integrated intensities, $I_{INT}$, corresponding to the radial and tangential scattering profiles while shearing at 26.9 °C and $\omega = 0.16$ rad/s.
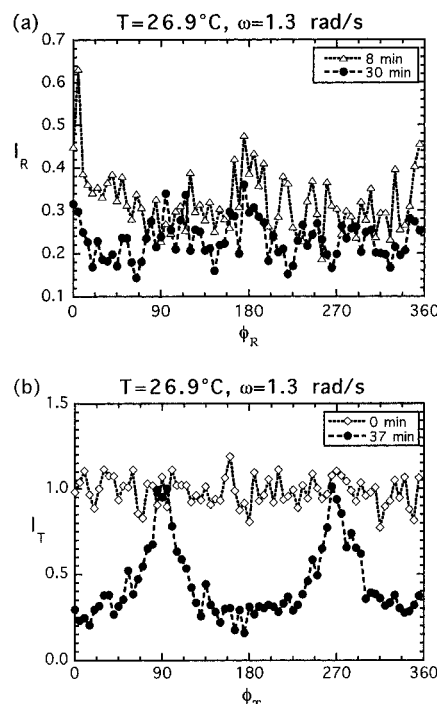




**Figure 11.** Evolution of normalized (a) radial and (b) tangential scattering with time while shearing at 26.9 °C with $\omega = 1.3$ rad/s.

**Effect of Frequency at $T = 26.9$ °C and the Undulation Instability.** In Figure 11 we show radial and tangential profiles at selected times at a frequency of 1.3 rad/s and $T = 26.9$ °C. After 37 min of shearing the intensity in all other angles except that corresponding to parallel lamellae have diminished to 0.2, while $I_T(\phi_T = 90°, 270°)$ remains at unity. We therefore see a weak parallel alignment as was the case at $T = 24.4$ °C and $\omega = 0.63$ rad/s (Figures 6−8). Again, we are forced to conclude that imposing a frequency of 1.3 rad/s at $T = 26.9$ °C results in a disordering of all grains except those with parallel orientation.

It is evident from Figures 9−11 that increasing the frequency at 26.9 °C leads to increased disorder. To study this trend further, we followed the reorganization of lamellae at $\omega = 5.0$ rad/s, keeping $T$ fixed at 26.9 °C. The resulting radial and tangential profiles at selected times are shown in Figure 12. After 3 min of shearing, we see a dramatic buildup of perpendicular lamellae. The value of $I_R(\phi_R = 0°, 180°)$ is 30 at this point, implying that the volume fraction of perpendicular lamellae after 3 min of shearing is increased by 3000%,
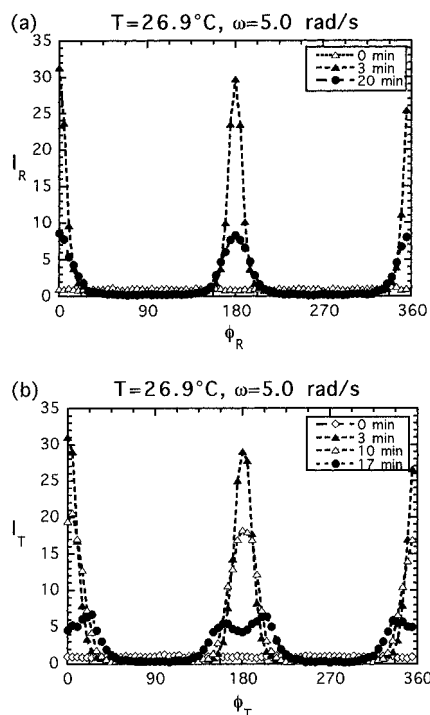
**Figure 12.** Evolution of normalized (a) radial and (b) tangential scattering with time while shearing at 26.9 °C with $\omega$ = 5.0 rad/s from $t$ = 0 to 20 min. The splitting from two peaks at $\phi_T$ = 0°, 180° to four peaks at $\phi_T$ = 20°, 160°, 200°, and 340° in the tangential profile is evidence for an undulation instability.
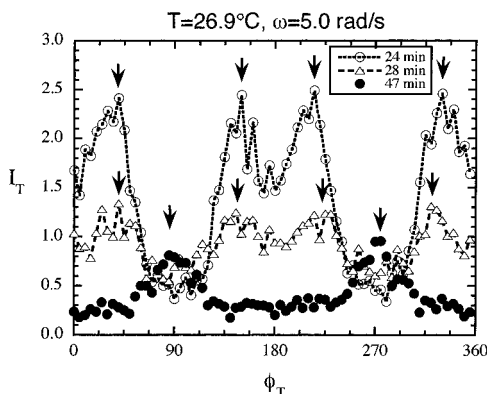


**Figure 13.** Evolution of normalized, tangential scattering with time while shearing at 26.9 °C with $\omega$ = 5.0 rad/s for $t \geq$ 24 min: (○) $t$ = 24 min, (△) $t$ = 28 min, (●) $t$ = 47 min. The arrows show the location of the scattering peaks corresponding to the dominant orientation of the lamellae.

relative to the isotropic state. This represents the best alignment that we were able to achieve in this sample. Unfortunately, this state was transient in nature. With time, the perpendicular lamellae disappeared and the alignment became weaker, as indicated by the decrease in scattering intensity with increasing time (Figure 12). The tangential profiles obtained toward the end of this run are shown on an expanded scale in Figure 13. Four scattering peaks were evident in the tangential configuration in the window 13 < $t$ < 32 min. At $t$ = 32 min, the four peaks disappeared, and gradually, two peaks at $\phi_T$ = 90° and 270° were obtained. These peaks are indicative of the parallel alignment, and as usual, they were poorly defined. The tangential scattering profile at $t$ = 47 min is also shown in Figure 13. The evolution of lamellar orientation at $T$ = 26.9 °C and $\omega$ = 5.0 rad/s is summarized in Figure 14 where we plot the time dependence of the intensities in the principal directions.
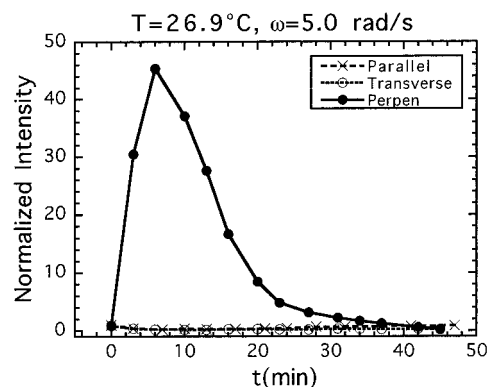


**Figure 14.** Time dependence of the normalized intensities in the principal directions at 26.9 °C with $\omega$ = 5.0 rad/s. As indicated in the text, these values reflect the fractional enhancement of the volume fraction of lamellae with normals in the corresponding, principal directions: (●) $I_R(\phi_R = 0°, 180°)$ or volume fraction of perpendicular lamellae estimated from the radial profiles, (○) $I_R(\phi_R = 90°, 270°)$ or volume fraction of transverse lamellae estimated from the radial profiles, (×) $I_T(\phi_T = 90°, 270°)$ or volume fraction of parallel lamellae estimated from the tangential profiles.
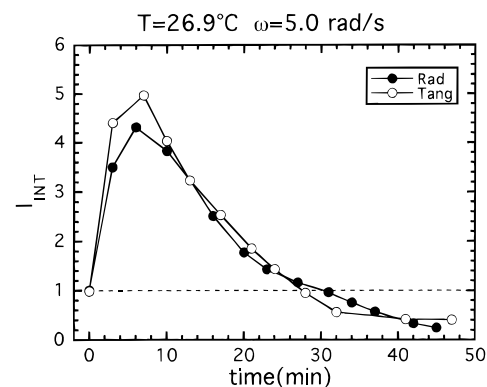


**Figure 15.** Time dependence of the integrated intensities, $I_{INT}$, corresponding to the radial and tangential scattering profiles while shearing at 26.9 °C and $\omega$ = 5.0 rad/s.

The buildup of perpendicular lamellae, followed by their destruction, is evident in these data. The time dependence of the integrated radial and tangential intensities, shown in Figure 15, confirms our conclusion of eventual shear disordering.

The events leading to the disordering of the perpendicular lamellae are clearly evident in the tangential profiles, shown in Figures 12b and 13. At early times ($t$ < 10 min) we see two peaks in $I_T$ at $\phi_T$ = 0° and 180°. This fact, in conjunction with the large magnitude of $I_T$, indicates the sample consisted of perfectly aligned (or nearly so), perpendicular lamellae. This is depicted in Figure 16a. As time progressed ($t \geq$ 13 min), these peaks split into four peaks. At $t$ = 17 min, for example, the peaks in the tangential profiles occur at $\phi_T$ = 20°, 160°, 200°, and 340° (see Figure 12b). This implies that the dominant directions of lamellar alignment are ±20° relative to the neutral direction. The symbol $\Delta\phi$ is used to represent the average difference between the values of $\phi_T$ of the four peaks and the neutral direction [(|20−0| + |340−360| + |160−180| + |200−180|)/4 = 20 = $\Delta\phi(t$ = 17 min)]. A schematic representation of the dominant lamellar orientation during this time is shown in Figure 16b. In Figure 17 we plot the time dependence of $\Delta\phi$. From $t$ = 10 min to $t$ = 28 min, the dominant orientation shifts away from the perpendicular orientation. The data in Figure 13 are consistent with the notion that the perpendicular lamellae are undergoing a buckling
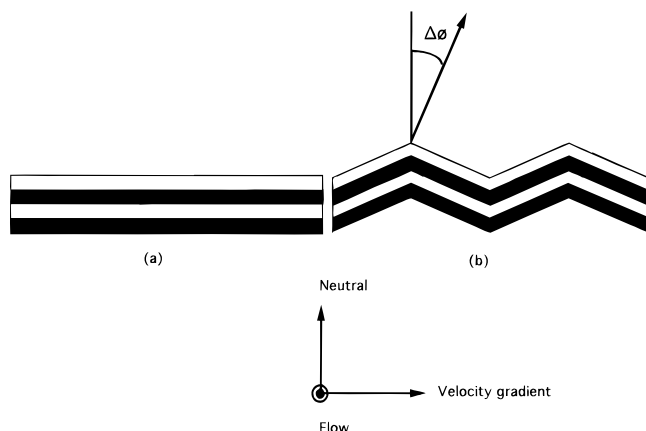
**Figure 16.** Schematic sketch of the dominant lamellar orientation at 26.9 °C and $\omega = 5.0$ rad/s at (a) early ($t < 13$ min) and (b) intermediate ($13 < t < 32$ min) times.
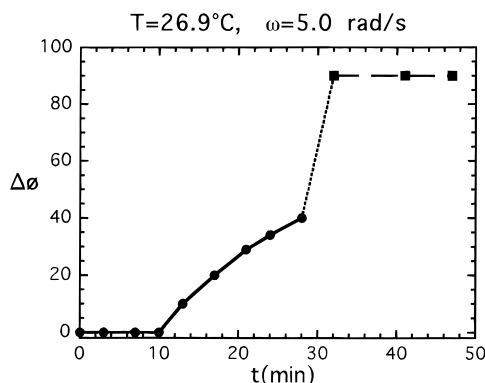


**Figure 17.** Plot of $\Delta\phi$ versus time at 26.9 °C with $\omega = 5.0$ rad/s. See text and Figure 16 for definition of $\Delta\phi$.
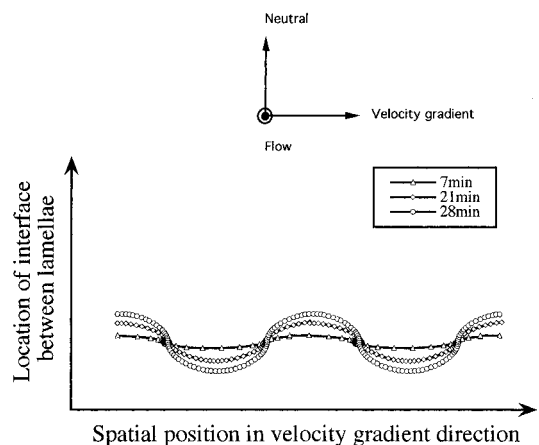


**Figure 18.** Time evolution of the interface between polystyrene and polyisoprene lamellae during the undulation instability, observed at 26.9 °C with $\omega = 5.0$ rad/s. See text for details regarding the construction of these curves.

transition. This interpretation assumes that grains with orientation $+\Delta\phi$ and $-\Delta\phi$ lie adjacent to each other. This seems to be reasonable because when four peaks in the tangential profile are evident, they are of roughly equal height (within experimental error). This implies that the volume fractions of grains with $+\Delta\phi$ and $-\Delta\phi$ orientations are equal. This observation, along with the fact that $\Delta\phi$ increases smoothly with time, is strong evidence for a buckling transition. It is difficult to imagine lamellae at random locations in the sample tilting in unison by $+\Delta\phi$ and $-\Delta\phi$. Note also that the buckling is confined to the velocity gradient−neutral plane; there are no indications of the buckling transition in the radial view (Figure 12a).

The sketches in Figure 16 are simplified versions of reality. The scattering intensities in the tangential configuration ($I_T$) at $\phi_T \neq \pm\Delta\phi$ are non-negligible. This indicates that there is a distribution of grain orientations which is peaked at $\pm\Delta\phi$. Thus, a more realistic view of the lamellae at $t \geq 13$ min is one where the lamellae undergo smooth undulations, rather that an abrupt buckling. The numerical value of $I_T(\phi_T)$ in Figures 12b and 13 is proportional to the instantaneous volume fraction of lamellae with normals oriented at an angle $\phi_T$ with respect to the neutral direction. Using this information we can reconstruct the shape of the undulating lamellae at various times. These results are shown in Figure 18 for $t = 7$, 21, and 28 min. The curves in Figure 18 indicate the location of the interface between polystyrene and polyisoprene lamellae, as viewed along the flow direction. The orientation of each line segment between two adjacent data points was obtained from the value of $\phi_T$; the normal to the line

segment is at an angle of $\phi_T$ to the vertical direction, which in Figure 18 corresponds to the neutral direction. The lengths of the line segments were obtained from the value of $I_T$ at that particular value of $\phi_T$. The tangential profiles should, in principle, have inversion symmetry with the incident beam ($|\mathbf{q}| = 0$) as the inversion center. Therefore, the line segment corresponding to a given value of $\phi_T$ was drawn such that its length was proportional to the mean of $I_T(\phi_T)$ and $I_T(\phi_T + 180°)$. Note that at $t = 7$ min we do not have a perfect horizontal line because the $I_T$ at $\phi_T = 90°$ and 270° are not identically zero. The SANS data provide no direct information about the wavelength of the undulation, and for simplicity, we have assumed it to be independent of time.

Undulations in low molecular weight, smectic A liquid crystals have been studied extensively. In a seminal paper, Helfrich recognized that, under quiescent conditions, lamellar phases formed in surfactant solutions were stabilized by undulations.[34] Subsequently, it was shown that undulation instabilities can be caused by external fields.[21] Theories by Fukuda and Onuki[35] and Wang[36] have shown that similar instabilities can occur in block copolymers. In a recent theoretical paper, Williams and MacKintosh[37] have shown that shear deformation can cause undulations in block copolymers lamellae. These calculations were restricted to strongly segregated block copolymers well-removed from an ODT (which is not the case in our study). It was found that lamellae in the parallel orientation would begin to show undulations when the shear stress exceeded a certain critical value. This work[37] provided a basis for the mechanism for destabilizing parallel lamellae, proposed by Koppi et al.[4] The undulations that we have observed in the SI(16−18)/DOP solution are qualitatively different from those reported in previous publications.[4,34−37] Here we find that lamellae in the perpendicular orientation exhibit a shear-induced, undulation instability. The field, in our case, is applied at the edges of the lamellae, and this gives rise to undulations.

**Flipping Lamellae by Changing Frequency.** We studied the response of the SI(16−18)/DOP solution to a step change in frequency at 26.9 °C. We first imposed a frequency of 0.16 rad/s which yielded perpendicular lamellae (see Table 1). The transformation of perpendicular to parallel lamellae was studied by increasing $\omega$ to 1.3 rad/s at $t = 39$ min. The measured radial and
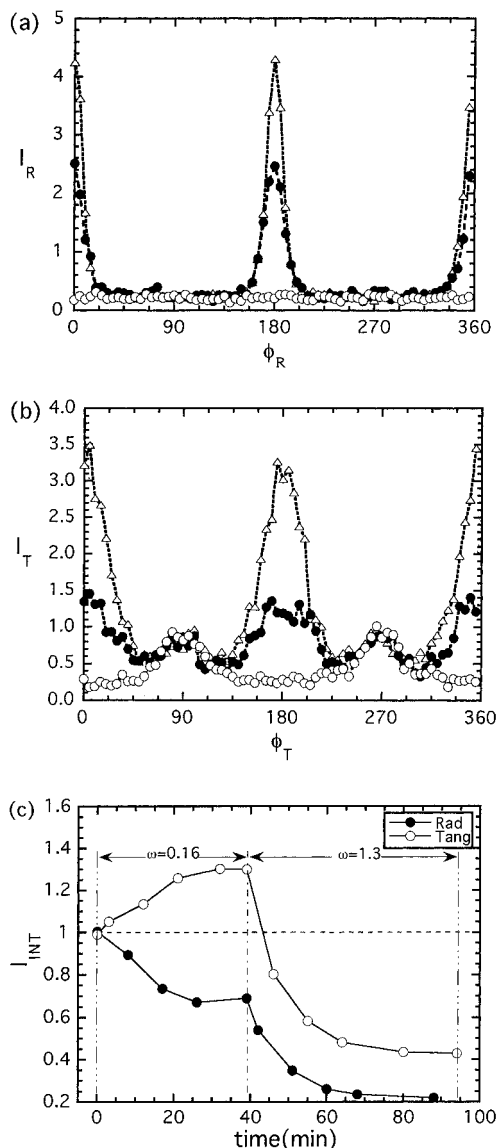
**Figure 19.** Evolution of normalized (a) radial and (b) tangential scattering with time at $T = 26.9$ °C after switching from $\omega = 0.16$ to 1.3 rad/s. The sample was quiescently quenched and sheared at $\omega = 0.16$ rad/s for 39 min to obtain the perpendicular alignment, the motor was stopped, and then $\omega$ was switched to 1.3 rad/s. This caused the lamellae to flip from the perpendicular to the parallel alignment: (a) ($\triangle$) $t = 39$ min, ($\bullet$) $t = 42$ min, and ($\bigcirc$) $t = 88$ min; (b) ($\triangle$) $t = 39$ min, ($\bullet$) $t = 46$ min, and ($\bigcirc$) $t = 94$ min. (c) Time dependence of the integrated intensities, $I_{INT}$, corresponding to the radial and tangential scattering profiles.

tangential profiles after switching frequencies are shown in Figures 19a,b. We find a monotonic decay of volume fraction of perpendicular lamellae, eventually leading to disorder. On the other hand, no change in the volume fraction of parallel lamellae was evident during this time. We do not find strong evidence for an undulation instability in this experiment, indicating that the decay of perpendicular lamellae can occur by a variety of mechanisms. The time dependence of the integrated intensities for this experiment is shown in Figure 19c. It is evident that the shear-disordered, parallel state at $T = 26.9$ °C and $\omega = 1.3$ rad/s is obtained, regardless of whether the sample is initially isotropic (Figure 11) or prealigned in the perpendicular state (Figure 19).

We also switched back from $\omega = 1.3$ to 0.6 rad/s, but the lamellar alignment was irreversible. Once the weakly aligned, parallel state was formed, decreasing

the frequency to 0.6 rad/s did not result in a well-aligned perpendicular state. This indicates that the weakly aligned state is more "stable". It is possible that the perpendicular state, obtained by applying $\omega = 1.3$ rad/s to the quiescent state, is a long-lived or trapped intermediate state. Similar irreversibility has been observed by others.[4]

## Comparison with Other Works and Concluding Remarks

The new conclusions of this work are captured by the data at $T = 26.9$ °C and $\omega = 5.0$ rad/s. We find that under these conditions, well-aligned, perpendicular lamellae disorder via an undulation instability. These conclusions are based on explicit determination of lamellar volume fractions in all three principal directions under shear flow. These results were obtained from a symmetric diblock copolymer sample, 8−10 °C below the order to disorder transition. This is a well-studied system,[2−9,16−21] yet neither shear-induced disordering nor undulation instabilities ever been observed in these systems. The question remains whether these phenomena are a common occurrence in other block copolymers. An important distinction between our samples and those studied by others is that we have studied concentrated solutions of block copolymers while others have studied block copolymer melts. An argument may therefore be made that the phenomena of shear disordering is somehow related to the presence of the solvent (DOP). In our previous work on a 65 wt % SI(11−17)/DOP solution, we found that reciprocating shear, similar to that used in this study,[38] produced nearly perfect, parallel lamellae[9] which showed no signs of shear-induced disorder. That solution had an ODT temperature of 35 ± 1 °C (identical with the one studied here), and it was also examined in the vicinity of 25 °C. It is therefore unlikely that the shear disordering is due, entirely, to the presence of the solvent.

We compare our findings with those of Gupta et al.,[6] who studied the alignment of an SI(10−10) melt under shear by birefringence. A transparent, parallel plate device was used to shear the sample, and the polarization of the light transmitted through the plates was measured. Thus only two principal directions (neutral and velocity) were accessible. Roughly speaking, the measured birefringence ($\Delta n$) is proportional to the volume fraction of perpendicular lamellae, and we can therefore compare this signal with the $I_T(\phi_T = 0°, 180°)$. We show data of Gupta et al. at 120 °C (which is 44 °C below the quiescent ODT), $\omega = 10$ rad/s, and $A = 80\%$. Under these conditions, Gupta et al. concluded that a pronounced intermediate state comprising perpendicular lamellae was formed, eventually giving way to parallel lamellae. We show their data in Figure 20. It is evident that the perpendicular lamellae disappear, and Gupta et al. concluded that they must be reorienting to the parallel state, which gives $\Delta n \approx 0$. However, as they recognized, the disordered state would also give $\Delta n \approx 0$. While the data of Gupta et al. are consistent with their conclusion, their data are also consistent with the conclusion that the perpendicular lamellae were disordered. We do not to wish reinterpret previous experiments.[6] We merely point out that shear disordering is not ruled out by these data. The data of Gupta et al. are compared with the measured time dependence of $I_T(\phi_T = 0°)$ obtained by us at $T = 26.9$ °C, $\omega = 5$ rad/s, and $A = 400\%$ in Figure 20.

We now address the other data on shear alignment of symmetric block copolymers, which was not obtained
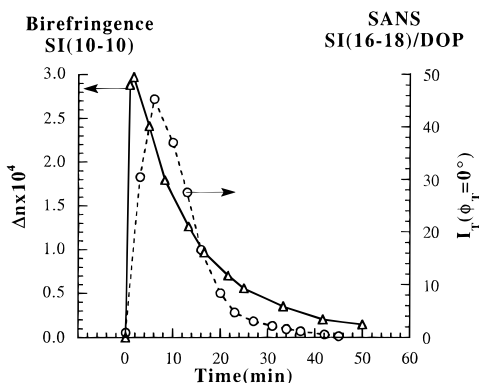
**Figure 20.** Comparison of SANS results reported here on the SI(16−18)/DOP solution ($T = 26.9$ °C, $\omega = 5.0$ rad/s) with birefringence results reported in ref 6 on an SI(10−10) melt ($T = 120$ °C, $\omega = 10.0$ rad/s). The measured signal in both experiments is proportional to the volume fraction of perpendicular lamellae.
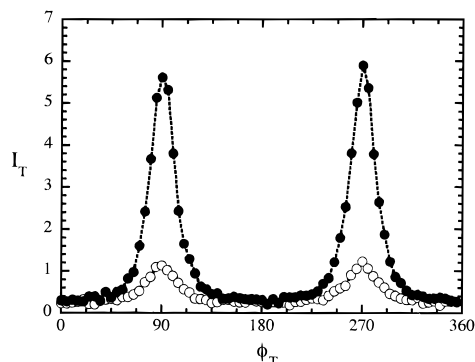


**Figure 21.** Reordering of the SI(16−18)/DOP solution under quiescent conditions, after the formation of the mostly disordered, parallel alignment: (○) tangential scattering profile at $T = 24.0$ °C after shearing at $\omega = 2.5$ rad/s. The shear field was then turned off, and the sample was slowly heated to 30 °C under quiescent conditions. The increase in the scattering at $\phi_T = 90°$ and 270° indicates the formation of well-aligned, parallel lamellae.

by *in-situ* measurements.[4,5,8] In such experiments, the shearing is stopped, and the sample is brought to room temperature, removed from the shear device, and then examined. Our SI(16−18)/DOP solution, in the temperature range of the shear experiments (24.4−26.9 °C), is well below the quiescent ODT. Therefore, when we stop shearing a sample that has been shear-disordered (i.e., weak parallel alignment), we expect the order to reappear. This is exactly what we observed. In Figure 21 we show the tangential profiles from mostly disordered, parallel lamellae, obtained just after shearing at $T = 24$ °C and $\omega = 2.5$ rad/s. We stopped shearing and examined the sample under quiescent conditions. A slow increase in the peak intensity was evident. We found that the ordering process could be accelerated by heating the sample to 30 °C, due to increased mobility at the higher temperature.[39] The scattering profile obtained after slowly heating the sample (over 40 min) from 24 to 30 °C is also shown in Figure 21. A 6-fold increase in $I_T(\phi_T = 90°$ and 270°) is evident, indicating the return of order. It is evident that the few ordered grains with parallel orientation, remaining after shearing at $T = 24$ °C and $\omega = 2.5$ rad/s, served as a template for the reordering. These experiments show that the structure of a block copolymer after shear and during shear can be qualitatively different. Thus, if shear disordering were occurring in the previous experiments,

postshear treatment may have caused the order to reappear.

Current theories on shear alignment in block copolymers[17−20] are inconsistent with our observation that applying shear fields can result in the disordering of lamellar grains, below the quiescent ODT. Due to symmetry considerations, it has been suggested that the effect of shear flow on all smectic A materials (low molecular weight materials and block copolymers) is similar.[19] Only shear ordering has been observed thus far in low molecular weight smectics.[40] In a recent theoretical paper, Ramaswamy proposed the possibility of shear-induced disordering of the lamellar phase in surfactant solutions.[41] This work is applicable to dilute lamellar phases, i.e., when the interlamellar spacing is much larger than the lamellar (membrane) thickness. We cannot use this theory to interpret our results because our lamellar systems are not dilute [lamellar spacing in SI(16−18)/DOP = 2(lamellar thickness)]. Our experiments indicate the need for a revised theory for shear alignment and shear ordering of block copolymers.

The discussion thus far has been limited to lamellae formed by diblock copolymers. Shear alignment of cylindrical phases formed by diblock and triblock copolymers has also been investigated.[10−15] Shear-induced ordering was observed over a wide range of conditions. There are, however, two exceptions[10,13] where shear-induced disordering was reported; they are as follows:

(1) In an earlier paper,[13] we reported shear-induced ordering at low shear rates and shear-induced disordering at high shear rates in a concentrated SI(8−22)/DOP solution with cylindrical morphology. However, these observations were made at a temperature that was 9 °C above the quiescent ODT.

(2) The experimental results of Winter et al. are more closely related to the present work.[10] They studied a cylindrical triblock copolymer melt [SIS(7-42-7), in our nomenclature] and found that the application oscillatory shear ($\omega = 0.01$ rad/s, $A = 400\%$), 10 °C below the quiescent ODT, caused the sample to disorder. It has been recognized that ordered structures formed by triblock copolymers have additional complexity due to the fact that the middle block can form loops or bridges.[14,42] Current experiments indicate that a substantial fraction (roughly 0.5) of the chains form bridges.[42] This is relevant because cylinders under shear always line up along the flow direction,[10−15] and bridges would therefore be unstable under large amplitude shear deformation. Since the current theories[17−20] on shear-ordering in block copolymers do not consider the presence of bridges, it is difficult to gauge the importance of this effect and its relationship to the shear-disordering result of Winter et al. Nevertheless, ref 10 contains the first evidence of shear-induced disorder in block copolymers.

## References and Notes

(1) Folkes, M. J.; Keller, A. *J. Polym. Sci., Polym. Phys. Ed.* **1976**, *14*, 833.

(2) Hadziioannou, G.; Skoulios, A. *Macromolecules* **1982**, *15*, 258.

(3) (a) Colby, R. H. *Curr. Opin. Colloid Interface Sci.* **1996**, *1*, 454. (b) Fredrickson, G. H.; Bates, F. S. *Annu. Rev. Mater. Sci.* **1996**, *26*, 501.

(4) Koppi, K. A.; Tirrell, M.; Bates, F. S.; Almdal, K.; Colby, R. H. *J. Phys. (France)* **1992**, *2*, 1941.

(5) (a) Larson, R. G.; Winey, K. I.; Patel, S. S.; Watanabe, H.; Bruinsma, R. *Rheol. Acta* **1993**, *32*, 245. (b) Winey, K. I.; Patel, S. S.; Watanabe, H. *Macromolecules* **1993**, *26*, 2542, 4373. (c) Patel, S. S.; Larson, R.; Winey, K. I.; Watanabe, H. *Macromolecules* **1995**, *28*, 4313.

(6) Gupta, V. K.; Krishnamoorti, R.; Kornfield, J. A.; Smith, S. D. *Macromolecules* **1995**, *28*, 4464.

(7) Gupta, V. K.; Krishnamoorti, R.; Chen, Z. R.; Kornfield, J. A.; Smith, S. D.; Satkowski, M. M.; Grothaus, J. T. *Macromolecules* **1996**, *29*, 875 and references therein.

(8) Zhang, Y.; Weisner, U.; Yang, Y.; Pakula, T.; Speiss, H. W. *Macromolecules* **1996**, *29*, 5427.

(9) (a) Balsara, N. P.; Hammouda, B. *Phys. Rev. Lett.* **1994**, *72*, 360. (b) Balsara, N. P.; Hammouda, B.; Kesani, P. K.; Jonnalagadda, S. V.; Straty, G. C. *Macromolecules* **1994**, *27*, 2566.

(10) Winter, H. H.; Scott, D. B.; Gronski, W.; Okamoto, S.; Hashimoto, T. *Macromolecules* **1993**, *26*, 7236.

(11) Almdal, K.; Bates, F. S.; Mortensen, K. *J. Chem. Phys.* **1992**, *96*, 9122.

(12) Morrison, F. A.; Mays, J. W.; Muthukumar, M.; Nakatani, A. I.; Han, C. C. *Macromolecules* **1993**, *26*, 5271.

(13) Balsara, N. P.; Dai, H. J. *J. Chem. Phys.* **1996**, *105*, 2942.

(14) Nakatani, A. I.; Morrison, F. A.; Douglas, J. F.; Mays, J. W.; Jackson, C. L.; Muthukumar, M.; Han, C. C. *J. Chem. Phys.* **1996**, *104*, 1589.

(15) Tepe, T.; Schulz, M. F.; Zhao, J.; Tirrell, M.; Bates, F. S. *Macromolecules* **1995**, *28*, 3008.

(16) Koppi, K. A.; Tirrell, M.; Bates, F. S. *Phys. Rev. Lett.* **1993**, *70*, 1449.

(17) Fredrickson, G. H. *J. Rheol.* **1994**, *38*, 1045.

(18) Goulian, M.; Milner, S. T. *Phys. Rev. Lett.* **1995**, *74*, 1775.

(19) Cates, M. E.; Milner, S. T. *Phys. Rev. Lett.* **1989**, *62*, 1856.

(20) Cates, M. E.; Marques, C. M. *J. Phys. (France)* **1990**, *51*, 1733.

(21) de Gennes, P. G.; Prost, J. *The Physics of Liquid Crystals*, 2nd ed.; Oxford: New York, 1993.

(22) Chandrasekhar, S. *Liquid Crystals* 2nd ed.; Cambridge: New York, 1992.

(23) Gido, S. P.; Thomas, E. L. *Macromolecules* **1994**, *27*, 6137 and references therein.

(24) Garetz, B. A.; Balsara, N. P.; Dai, H. J.; Wang, Z.; Newstein, M. C.; Majumdar, B. *Macromolecules* **1996**, *29*, 4679 and references therein.

(25) Diat, O.; D. Roux, D.; Nallet, F. *J. Phys. II (France)* **1993**, *3*, 1427.

(26) Lin, C. C.; Jonnalagadda, S. V.; Kesani, P. K.; Dai, H. J.; Balsara, N. P. *Macromolecules* **1994**, *27*, 7769.

(27) Amundson, K. R.; Helfand, E.; Patel, S. S.; Quan, X.; Smith, S. S. *Macromolecules* **1992**, *25*, 1935.

(28) Balsara, N. P.; Perahia, D.; Safinya, C. R.; Tirrell, M.; Lodge, T. P. *Macromolecules* **1992**, *25*, 3896.

(29) Fredrickson, G. H.; Leibler, L. *Macromolecules* **1989**, *22*, 1238.

(30) Leibler, L. *Macromolecules* **1980**, *13*, 1602.

(31) Fredrickson, G. H.; Helfand, E. *J. Chem. Phys.* **1987**, *87*, 697.

(32) Perahia, D.; Vacca, G.; Patel, S. S.; Dai, H. J.; Balsara, N. P. *Macromolecules* **1994**, *27*, 7645.

(33) Amundson, K.; Helfand, H. *Macromolecules* **1993,** *26*, 1324.

(34) Helfrich, W. *Z. Naturforsch.* **1978**, *33a*, 305.

(35) Fukuda, J.; Onuki, A. *J. Phys. II (France)* **1995**, *5*, 1107.

(36) Wang, Z. G. *J. Chem. Phys.* **1994**, *100*, 2298.

(37) Williams, D. M. R.; MacKintosh, F. C. *Macromolecules* **1994**, *27*, 7677.

(38) There is a minor difference in the shearing conditions in the two experiments. We used an amplitude of 400% in this work on SI(16−18)/DOP and 200% in the previous work[9] on SI(11−17)/DOP. We started our studies on the SI(16−18)/DOP with 200% strain and found results similar to those reported in this paper. Our original intent was to obtain well-aligned states, so we increased the strain to 400%, with the hope of reducing imperfection density. Of course, this did not turn out to be the case.

(39) The quiescent ordering kinetics in this solution, after quenching from the disordered state to temperatures between 24 and 35 °C, were studied using the local birefringence method. The rate of growth of the ordered phase was maximum at 30 °C (A. Krishnan and N. P. Balsara, unpublished results). During our SANS experiment, the sample was heated to 30 °C to save precious time on the neutron machine. The slow reordering kinetics at 24 °C are not completely understood, especially after shear disordering, and are the subject of ongoing research.

(40) (a) Safinya, C. R.; Sirota, E. B.; Plano, R. J. *Phys. Rev. Lett.* **1991**, *66*, 1986. (b) Bruinsma, R. F.; Safinya, C. R. *Phys. Rev. A* **1991**, *43*, 5377. (c) Safinya, C. R.; Sirota, E. B.; Bruinsma, R. F.; Jeppesen, C.; Plano, R. J.; Wenzel, L. J. *Science* **1993**, *261*, 588.

(41) Ramaswamy, S. *Phys. Rev. Lett.* **1992**, *69*, 112.

(42) Watanabe, H. *Macromolecules* **1995**, *28*, 5006.

(43) Certain equipment and instruments or materials are identified in this paper in order to adequately specify the experimental details. Such identification does not imply recommendation by the National Institute of Standards and Technology, nor does it imply the materials are necessarily the best available for the purpose.